http://dx.doi.org/10.5012/bkcs.2012.33.4.1303

The Co-luminescence Groups of Sm-La-pyridyl Carboxylic Acids and the Binding Characteristics between the Selected Doped Complex and Bovine Serum Albumin

Zhengfa Yang, Ruiren Tang,* and Chunhua Tang

School of Chemistry and Chemical Engineering, Central South University, Changsha, 410083, P. R. China
**E-mail: trr@mail.csu.edu.cn*
Received December 4, 2011, Accepted January 29, 2012

A novel ligand *N,N'*-(2,6-pyridinedicarbonyl)bis[*N*-(carboxymethyl)] (**L**$_1$) was designed and synthesized. Four co-luminescence groups of Sm-La-pyridyl carboxylic acids systems were researched, which are $K_4Sm_{(1-x)}La_x$(**L**$_1$)$Cl_3 \cdot y_1H_2O$, $K_4Sm_{(1-x)}La_x$(**L**$_2$)$Cl_3 \cdot y_2H_2O$, $K_6Sm_{2(1-x)}La_{2x}$(**L**$_3$)$Cl_6 \cdot y_3H_2O$, $K_4Sm_{(1-x)}La_x$(**L**$_4$)$Cl_3 \cdot y_4H_2O$. The results indicated the addition of La(III) could sensitize the luminescence of Sm(III) obviously in a certain range, enhancing emission intensity of Sm-pyridyl carboxylic acids relative to the undoped ones. The optimal mole percentages of La(III) in the mixed ions for **L**$_1$, **L**$_2$, **L**$_3$, **L**$_4$ were confirmed to be 0.6, 0.5, 0.3, 0.6, respectively. The mechanism of the fluorescence enhancement effect was discussed in detail. Furthermore, the binding interaction of $K_4Sm_{0.4}La_{0.6}$(**L**$_4$)$Cl_3 \cdot 5H_2O$ with bovine serum albumin (BSA) have been investigated due to its potential biological activity. The binding site number n was equal to 1.0 and binding constant K_a was about 2.5×10^5 L·mol^{-1}.

Key Words : Synthesis, Pyridine derivate, Lanthanide complex, Co-luminescence, Bovine serum albumin

Introduction

Luminescent rare earth organic complexes are of both fundamental and technical interest due to their characteristic luminescence properties, such as extremely sharp emission bands, long lifetime, and potential high internal quantum efficiency.[1-3] Nevertheless, the Ln(III) complexes usually give weak luminescence due to the weak absorption coefficient of the parity-forbidden f-f transitions which limits their practical application considerably. An effective approach to increase the luminescent efficiency is to modify the complexes with different kinds of highly absorbent chelating ligands that have broad and intense absorption bands,[4,5] which served as efficient sensitizers.[6] Besides, great interests have been paid on rare-earth ions co-luminescence effect, a fluorescence enhancement phenomenon which was first found and studied by Yang *et al.* in 1986.[7-9] According to this method, the addition of certain lanthanideions, such as La^{3+}, Lu^{3+}, Gd^{3+}, Y^{3+}, and Tb^{3+}, could greatly enhance the luminescence intensity of the Eu^{3+}, Tb^{3+}, and Sm^{3+} chelates in solution. The co-luminescence effect which involves an intermolecular energy transfer process has become an important way to improve the luminescence detection sensitivity of lanthanide ions. Also, rare-earth co-luminescence compounds have received great interest because of their important roles in the study of luminescent materials, NMR shift reagents and biological systems.[10] Over the past few years, our research groups have synthesized a series of chelating ligands **L**$_2$-**L**$_4$ (the structures of **L**$_1$, **L**$_2$, **L**$_3$, **L**$_4$ are showed in Scheme 1) and the luminescence properties of their lanthanide complexes were investigated by us.[11-13] Recently, we have turned our attention to rare-earth doped co-luminescence effect. The structures of **L**$_1$-**L**$_4$ all contain pyridine-2,6-dicarboxylic acid unit and have many coordination sites. Also, the coordination systems of the ligands **L**$_1$-**L**$_4$ are very unique. So, it is meaningful to study the four co-luminescence systems.

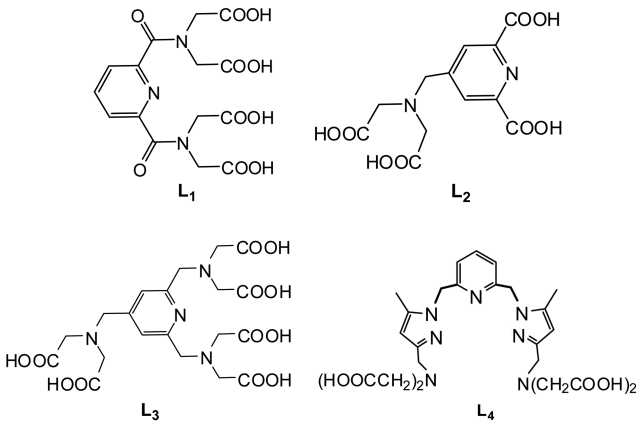

Scheme 1. The structures of **L**$_1$, **L**$_2$, **L**$_3$, **L**$_4$.

As far as we know, Sm(III) and La(III) own excellent drug activity, Sm(III) acetate, for instance, can be used as anticoagulant, La-complexes have been developed to be antidizziness, antiemetic, especially as antipyretic, owing to the effective function of inhibition the growth of epiphytes and bacteria.[14] The structure of **L**$_4$ contains pyridine and pyrazole rings, which are indispensable in many drug molecules. As is well known, serum albumins are the most abundant proteins in circulatory system, playing the most important physiological role in transportation of numerous exogenous and endogenous ligands, such as drugs in the bloodstream to their target organs.[15] So, it is very meaningful to explore the action mode between $K_4Sm_{0.4}La_{0.6}$(**L**$_4$)$Cl_3 \cdot 5H_2O$ and bovine

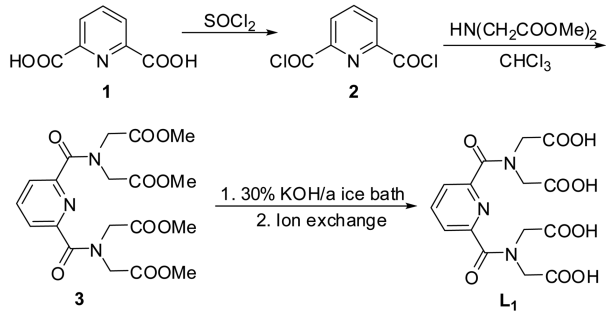

Scheme 2. The synthetic route of ligand $\mathbf{L}_1$.

serum albumin (BSA), which can provides a theoretical basis for their potential medicinal value.

In our work, a novel ligand, *N,N′*-(2,6-pyridinedicarbonyl)bis[*N*-(carboxymethyl)] ($\mathbf{L}_1$) was designed and synthesized starting from pyridine-2,6-dicarboxylic acid (**1**). $\mathbf{L}_2$, $\mathbf{L}_3$, $\mathbf{L}_4$ was prepared following literature methods.[11-13] Based on the rare-earth ions co-luminescence effect, four potential co-luminescence systems, *i.e.*, $K_4Sm_{(1-x)}La_x(\mathbf{L}_1)Cl_3{\cdot}y_1H_2O$, $K_4Sm_{(1-x)}La_x(\mathbf{L}_2)Cl_3{\cdot}y_2H_2O$, $K_6Sm_{2(1-x)}La_{2x}(\mathbf{L}_3)Cl_6{\cdot}y_3H_2O$, $K_4Sm_{(1-x)}La_x(\mathbf{L}_4)Cl_3{\cdot}y_4H_2O$ (x is the mole fraction of La(III) in the mixed ions, the value is 0, 0.1, 0.2, 0.3, 0.4, 0.5, 0.6, 0.7, 0.8, 0.9, 1.0, respectively; y_1, y_2, y_3, y_4 are plus integer), were studied to investigate the co-luminescence phenomenon between Sm(III) and La(III) with different pyridyl carboxylic acid ligands. Then the binding interaction of the select complex $K_4Sm_{0.4}La_{0.6}(\mathbf{L}_4)Cl_3{\cdot}5H_2O$ and BSA was carried out by fluorescence spectrum due to its potential biological activity, which showed the reference value for a model of application for drug design. The synthetic route of $\mathbf{L}_1$ was expressed in Scheme 2.

Experimental

Materials and Methods. The buffer Tris was purchased from Acros (Geel, Belgium). Tris-HCl buffer solution (pH = 7.4) was given *via* adding dropwise HCl (0.1 mol·L^{-1}) to Tris solution (0.1 mol·L^{-1}). By means of dissolving $K_4Sm_{0.4}La_{0.6}(\mathbf{L}_4)Cl_3{\cdot}5H_2O$ in water, then diluting it to the desired concentration, the working solution of the complex was obtained. The stock solution of BSA (purity ≥ 99%, purchased from Sino-Biotechnology Company, Shanghai, China) was prepared to be the concentration of 1.0×10^{-6} mol·L^{-1} by dissolving it in water, and kept it in the dark at 0-4 °C. 0.9% NaCl solution was used to maintain the ionic strength. Other chemicals were of A.R. grade and used without further purification. Water used in this study was doubly deionized.

All reactions were monitored by TLC on silica-gel F-254 plates (Merck) with detection under UV light. Elemental analysis was carried out by a PerkinElmer 2400 elemental analyzer; Melting points were determined on a XR-4 apparatus (thermometer uncorrected); Infrared spectra (4000-400 cm^{-1}) were recorded with samples as KBr discs using a Nicolet NEXUS 670 FT-IR spectrophotometer; The excitation and emission spectra were recorded on a Hitich F-4500 luminescence spectrophotometer. The luminescence data for each complexes were determined in the solid state at room temperature (The width of emission and excitation slit was 2.5 nm for Tb(III) complex, 5 nm for all other coordinated compounds, the voltage of photomultiplier tube was 700 V); ^{1}H-NMR was measured with a Bruker-500MHz nuclear magnetic resonance spectrometer with $CDCl_3$ or D_2O as solvent and TMS as internal reference.

Preparation of $\mathbf{L}_1$.

Synthesis of 2,6-Pyridinedicarbonyl Dichloride (2): 1 (10 mmol) was treated with thionyl chloride (20 mL) and one drop of *N*,*N*-dimethylformamide, then the mixture was refluxed at 70 °C for 4 hours. The excess thionyl chloride was removed by evaporation under reduced pressure. Residual thionyl chloride was removed by co-evaporation with 30 mL of anhydrous benzene to afford the corresponding diacid chloride **2**. This crude product was used in the following step without further purification.

Synthesis of *N,N′*-(2,6-Pyridinedicarbonyl)bis[*N*-(methoxyacetyl)] (3): Dimethyl iminodiacetate (1.288 g, 8 mmol) and 1 mL triethylamine were added into **2** (0.816 g, 4 mmol), which dissolved in 50 mL of $CHCl_3$. The mixture was refluxed for 2 h with stirring. After the solvent was evaporated, the crude product was obtained. The oily residue was purified by silica gel column chromatography using petroleum ether and ethyl acetate mixture (2:8, v:v) as eluent to give a white powder **3** (1.71 g, 94.1%). mp 127-128 °C; Anal. Calcd. for $C_{19}H_{23}N_3O_{10}$: C 50.33, H 5.08, N 9.27. Found: C 50.23, H 5.04, N 9.37%. IR (KBr): *v* 3000, 2957, 1737, 1634, 1581, 1200, 1004 cm^{-1}. ^{1}H NMR ($CDCl_3$, 500 MHz) δ 7.95 (m, Py-3,5, 2H), 7.85 (t, *J* = 7.80 Hz, Py-4, 1H), 4.35 (s, N-CH_2, 8H), 3.72 (s, -CH_3, 12H). EI-MS: *m/z* 453.3 [M]$^+$.

Synthesis of *N,N′*-(2,6-Pyridinedicarbonyl)bis[*N*-(carboxymethyl)] ($\mathbf{L}_1$): 2.5 mL of aqueous KOH (30%) was added to 10 mL of CH_3OH solution containing 1.539 g (3.4 mmol) **3** with stirring in an ice bath for 5 h. Then, the solvent was evaporated to give a yellow oily residue, which was purified using a 732 cation resin column to give a colorless solid $\mathbf{L}_1$ (1.22 g, 90.3%). mp 118-119 °C. Anal. Calcd. for $C_{15}H_{15}N_3O_{10}$: C 45.34, H 3.78, N 10.58. Found: C 45.33, H 3.74, N 10.51%. IR (KBr): *v* 3434, 2996, 1732, 1634, 1487, 1191, 1018 cm^{-1}. ^{1}H NMR (D_2O, 500 MHz) δ 8.12 (t, *J* = 7.50 Hz, Py-3,5, 2H), 7.82 (d, *J* = 7.80 Hz, Py-4, 1H,), 4.33 (s, N-CH_2, 8H). EI-MS: *m/z* 397.1[M]$^+$.

Synthesis of the Potential Co-luminescence Systems of $K_4Sm_{(1-x)}La_x(L_1)Cl_3{\cdot}y_1H_2O$, $K_4Sm_{(1-x)}La_x(L_2)Cl_3{\cdot}y_2H_2O$, $K_6Sm_{2(1-x)}La_{2x}(L_3)Cl_6{\cdot}y_3H_2O$, $K_4Sm_{(1-x)}La_x(L_4)Cl_3{\cdot}y_4H_2O$ (x = 0, 0.1, 0.2, 0.3, 0.4, 0.5, 0.6, 0.7, 0.8, 0.9, 1.0, respectively; y_1, y_2, y_3, y_4 are plus integer). To the water solution of $\mathbf{L}_1$, $\mathbf{L}_2$, $\mathbf{L}_3$, $\mathbf{L}_4$, the mixed solution of $SmCl_3$ and $LaCl_3$ (The mole fractions of La(III) in the mixed ions are 0, 0.1, 0.2, 0.3, 0.4, 0.5, 0.6, 0.7, 0.8, 0.9, 1.0, respectively) was added. The pH value of the solution was adjusted to 6.0 by dropwise addition of aqueous KOH (5%), and the mixture was stirred at 60 °C for 12 h. The resulting precipitate was collected by filtration, washed three times with ethanol and

chloroform mixture (1:1, v:v), dried and purified by recrystallization from a methanol-water mixture.

Results and Discussion

Elemental Analyses. The compositions of the doped complexes with the maximum fluorescence intensity were confirmed by elemental analyses. The elemental analyses results of C, H, and N are in accordance with the theoretical values calculated, indicated that the composition of the complexes are $K_4Sm_{0.4}La_{0.6}(\mathbf{L}_1)Cl_3{\cdot}6H_2O$, $K_4Sm_{0.5}La_{0.5}(\mathbf{L}_2)Cl_3{\cdot}11H_2O$, $K_6Sm_{1.4}La_{0.6}(\mathbf{L}_3)Cl_6{\cdot}8H_2O$, $K_4Sm_{0.4}La_{0.6}(\mathbf{L}_4)Cl_3{\cdot}5H_2O$ (Table 1).

FT-IR Spectra. The FT-IR spectra of $K_4Sm_{0.4}La_{0.6}(\mathbf{L}_1)Cl_3{\cdot}6H_2O$, $K_4Sm_{0.5}La_{0.5}(\mathbf{L}_2)Cl_3{\cdot}11H_2O$, $K_6Sm_{1.4}La_{0.6}(\mathbf{L}_3)Cl_6{\cdot}8H_2O$, $K_4Sm_{0.4}La_{0.6}(\mathbf{L}_4)Cl_3{\cdot}5H_2O$ are offered in this paper (Figure 1). Table 2 gives the characteristic infrared absorption bands of the free **L** and its complexes, which are useful for suggesting the mode of coordination of ligands. Regarding to $K_4Sm_{(1-x)}La_x(\mathbf{L}_1)Cl_3{\cdot}y_1H_2O$, $K_4Sm_{(1-x)}La_x(\mathbf{L}_2)Cl_3{\cdot}y_2H_2O$, $K_6Sm_{2(1-x)}La_{2x}(\mathbf{L}_3)Cl_6{\cdot}y_3H_2O$, $K_4Sm_{(1-x)}La_x(\mathbf{L}_4)Cl_3{\cdot}y_4H_2O$ (x = 0, 0.1, 0.2, 0.3, 0.4, 0.5, 0.6, 0.7, 0.8, 0.9, 1.0, respectively; y_1, y_2, y_3, y_4 are plus integer) with the specific ligand, the

Table 1. Composition analytical data for the complexes

Complexes	C	H	N
	Found (calc.)	Found (calc.)	Found (calc.)
$K_4Sm_{0.4}La_{0.6}(\mathbf{L}_1)Cl_3{\cdot}6H_2O$	19.49 (19.85)	1.24 (1.22)	4.77 (4.63)
$K_4Sm_{0.5}La_{0.5}(\mathbf{L}_2)Cl_3{\cdot}11H_2O$	15.98 (15.77)	0.85 (0.88)	3.09 (3.06)
$K_6Sm_{1.4}La_{0.6}(\mathbf{L}_3)Cl_6{\cdot}8H_2O$	17.33 (17.24)	1.46 (1.45)	4.09 (4.02)
$K_4Sm_{0.4}La_{0.6}(\mathbf{L}_4)Cl_3{\cdot}5H_2O$	29.01 (28.60)	2.64 (2.59)	9.41 (9.34)

Table 2. Characteristic IR bands (cm^{-1}) of the ligand and its complexes

Sample	ν(OH)	ν(C=O) of carboxyl	ν_{as} (COO-)	ν_s (COO-)
$\mathbf{L}_1$	3434	1732		
$K_4Sm_{0.4}La_{0.6}(\mathbf{L}_1)Cl_3{\cdot}6H_2O$			1587	1395
$\mathbf{L}_2$	3445	1721		
$K_4Sm_{0.5}La_{0.5}(\mathbf{L}_2)Cl_3{\cdot}11H_2O$			1594	1424
$\mathbf{L}_3$	3495	1746		
$K_6Sm_{1.4}La_{0.6}(\mathbf{L}_3)Cl_6{\cdot}8H_2O$			1590	1411
$\mathbf{L}_4$	3567	1746		
$K_4Sm_{0.4}La_{0.6}(\mathbf{L}_4)Cl_3{\cdot}5H_2O$			1598	1407

ν_{as}, asymmetric; ν_s, symmetric.

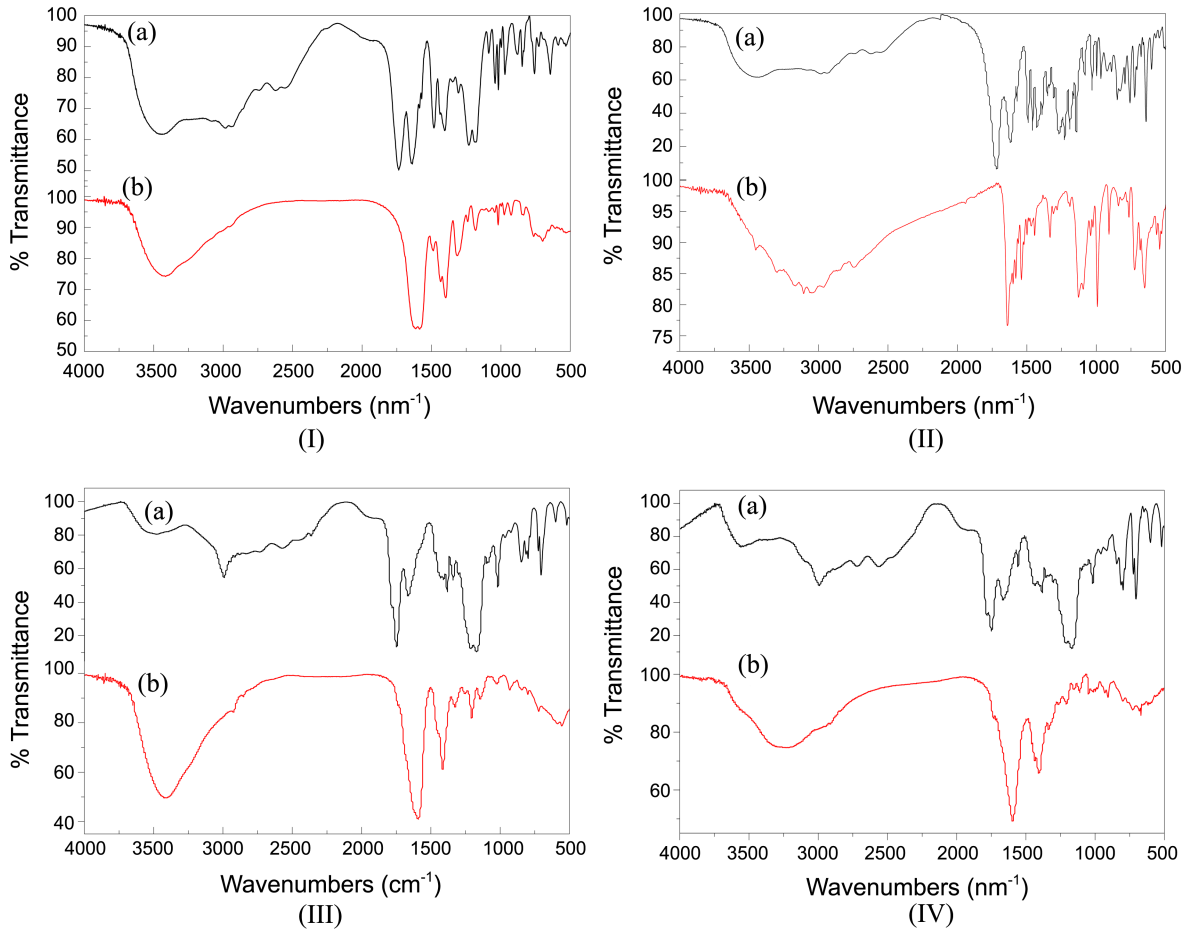

Figure 1. FT-IR spectra of Ia $\mathbf{L}_1$, Ib $K_4Sm_{0.5}La_{0.5}(\mathbf{L}_1)Cl_3{\cdot}6\ H_2O$, IIa $\mathbf{L}_2$, IIb $K_4Sm_{(1-x)}La_x(\mathbf{L}_2)Cl_3{\cdot}11H_2O$, IIIa $\mathbf{L}_3$, IIIb $K_6SmLa(\mathbf{L}_3)Cl_6{\cdot}8H_2O$ and IVa $\mathbf{L}_4$, IVb $K_4Sm_{0.5}La_{0.5}(\mathbf{L}_4)Cl_3{\cdot}5H_2O$.

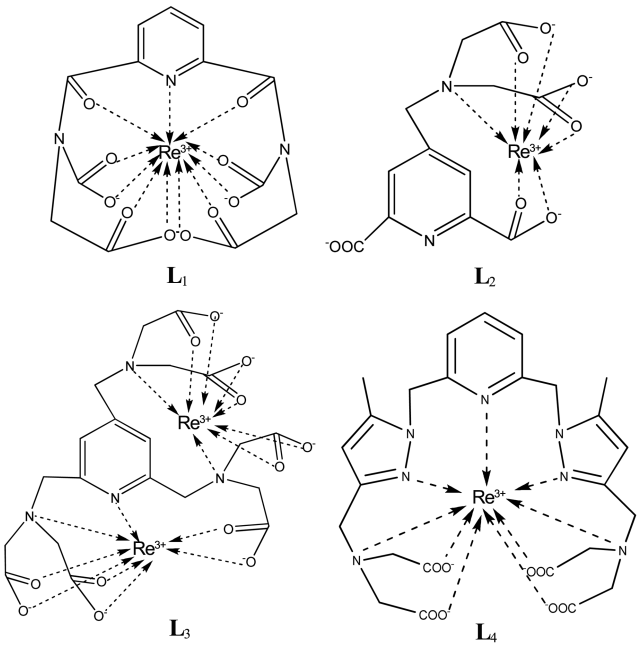

Scheme 3. The probable structures of these complexes.

spectra are similar with the different mole fractions of La(III), which implies that they are structurally alike with each other. While in comparison with their corresponding free ligand, the FT-IR spectra of the complexes are changed greatly, indicating that the coordination between metal and ligand is pretty good. According to FT-IR spectra and literature,[11-13] we suspect that the chemical structure of the complexes may be like this (Scheme 3):

Luminescence Properties.

Effect of La(III) Amount on the Emission Spectra: The emission spectra of $K_4Sm_{(1-x)}La_x(\mathbf{L}_1)Cl_3{\cdot}y_1H_2O$, $K_4Sm_{(1-x)}La_x(\mathbf{L}_2)Cl_3{\cdot}y_2H_2O$, $K_6Sm_{2(1-x)}La_{2x}(\mathbf{L}_3)Cl_6{\cdot}y_3H_2O$, $K_4Sm_{(1-x)}La_x(\mathbf{L}_4)Cl_3{\cdot}y_4H_2O$ (x = 0, 0.1, 0.2, 0.3, 0.4, 0.5, 0.6, 0.7, 0.8, 0.9, 1.0, respectively; y_1, y_2, y_3, y_4 are plus integer), are shown in Figure 2, and four systems all emit characteristic fluorescence of Sm(III) ion with excitation at 236 nm. The characteristic fluorescence intensity of Sm(III) gradually enhanced with the increase of the molar fractions of foreign inertia ion La(III) at a certain degree, however, the fluorescence intensity of four groups decreased with the increasing contents of La(III). To achieve the maximum luminous intensity, the optimal molar percentages of the doped La(III) in the total ions for different ligands are different. As is shown below, the shape of the bands is changed to cope with different ligands, which may be attributed to the energy difference between the ligand triplet state and the singlet excited state of rare earth ions. But the addition of doped ions does not change spectral shape for the same ligand.

Those above prove that foreign ions La(III) can sensitize Sm-pyridyl carboxylic acids within certain extent, in other words, there is co-luminescence effect between Sm(III) and

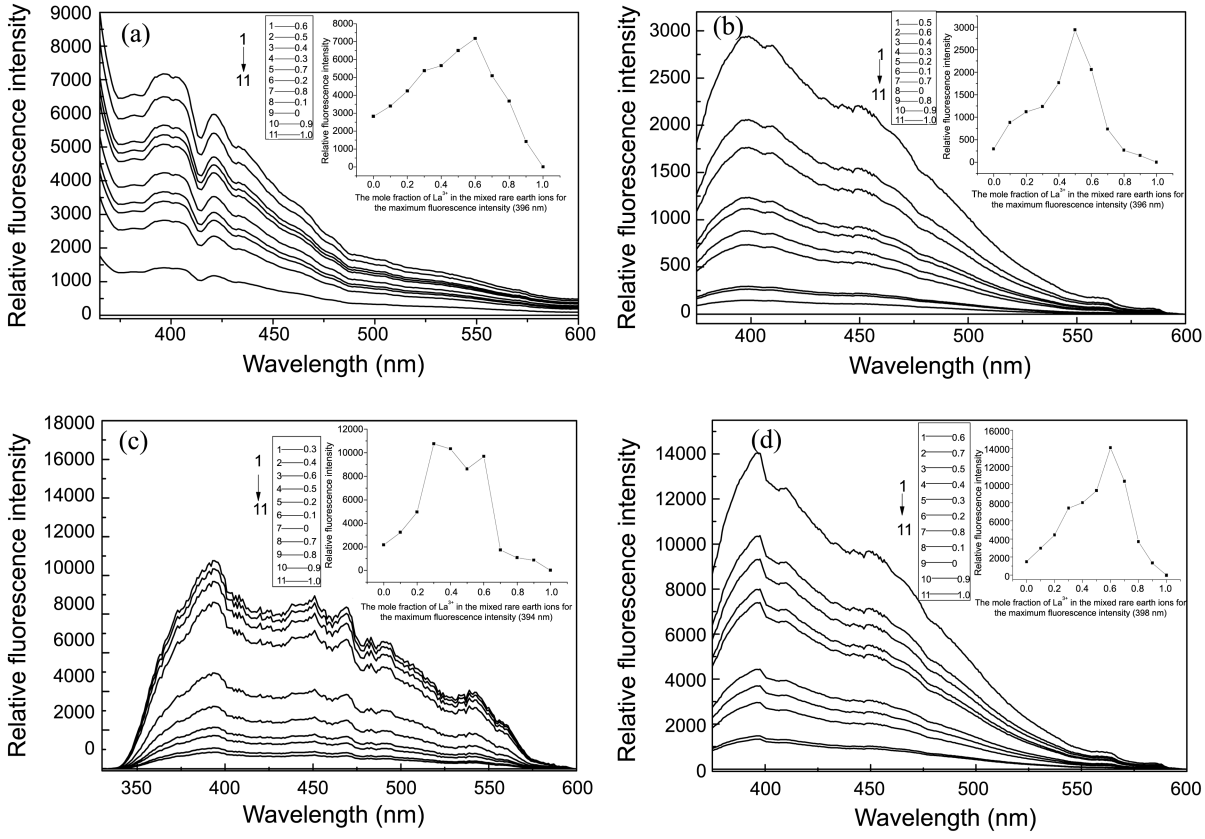

Figure 2. The emission spectra and maximum fluorescence intensity of the $K_4Sm_{(1-x)}Lax(\mathbf{L}_1)Cl_3{\cdot}y_1H_2O$ (a), $K_4Sm_{(1-x)}La_x(\mathbf{L}_2)Cl_3{\cdot}y_2H_2O$ (b), $K_6Sm_{2(1-x)}La_{2x}(\mathbf{L}_3)Cl_6{\cdot}y_3H_2O$ (c) and $K_4Sm_{(1-x)}La_x(\mathbf{L}_4)Cl_3{\cdot}y_4H_2O$ (d) (x = 0, 0.1, 0.2, 0.3, 0.4, 0.5, 0.6, 0.7, 0.8, 0.9, 1.0, respectively, y_1, y_2, y_3, y_4 is plus integer) versus contents of La(III).

La(III). In regard of the $K_4Sm_{(1-x)}La_x(\mathbf{L}_1)Cl_3{\cdot}y_1H_2O$, $K_4Sm_{(1-x)}La_x(\mathbf{L}_2)Cl_3{\cdot}y_2H_2O$, $K_6Sm_{2(1-x)}La_{2x}(\mathbf{L}_3)Cl_6{\cdot}y_3H_2O$, $K_4Sm_{(1-x)}La_x(\mathbf{L}_4)Cl_3{\cdot}y_4H_2O$ (x = 0, 0.1, 0.2, 0.3, 0.4, 0.5, 0.6, 0.7, 0.8, 0.9, 1.0, respectively; y_1, y_2, y_3, y_4 are plus integer), the maximum fluorescence intensity is up to 7176, 2939, 10760, 14043 with an increase of 2.54, 9.03, 4.00, 8.48 times relative to the undoped compounds, respectively. Furthermore, the optimal mole percentages of La(III) in the mixed ions among the $K_4Sm_{(1-x)}La_x(\mathbf{L}_1)Cl_3{\cdot}y_1H_2O$, $K_4Sm_{(1-x)}La_x(\mathbf{L}_2)Cl_3{\cdot}y_2H_2O$, $K_6Sm_{2(1-x)}La_{2x}(\mathbf{L}_3)Cl_6{\cdot}y_3H_2O$, $K_4Sm_{(1-x)}La_x(\mathbf{L}_4)Cl_3{\cdot}y_4H_2O$ (x = 0, 0.1, 0.2, 0.3, 0.4, 0.5, 0.6, 0.7, 0.8, 0.9, 1.0, respectively; y_1, y_2, y_3, y_4 are plus integer) are 0.6, 0.5, 0.3, 0.6, respectively. The results prove that the ligands we studied have a great influence on luminescence properties of co-luminescence systems. As is stated above, La(III) sensitizes Sm-$\mathbf{L}_2$ system to a higher degree compared to other three groups, but the maximum fluorescence intensity (2939) is comparatively low. The ligands $\mathbf{L}_1$, $\mathbf{L}_3$, $\mathbf{L}_4$ all can sensitize Sm(III) effectively on account of their larger conjugated systems and more coordination sites, especially for $\mathbf{L}_4$. The introduction of pyrazole units helps to form the rigid planar structure, enlarging the π-conjugated system of the ligand, which exhibits strong light-harvesting potential to enhance the emission intensity of metal ions. Moreover, the special structure of $\mathbf{L}_4$ can induce the spheroidal structure of the complexes, which can shield the interference of solvent molecules, and also improve the efficiency of ligand-to-metal energy transfer; hence $\mathbf{L}_4$ is the most effective sensitizer to rare-earth ions of the four ligands.

Luminescence Enhancement Mechanism in Solid State: It is generally believed that the fluorescence enhancement phenomenon was confirmed the structures of the complexes and intramolecular energy transfer, and related to energy transfer between neighboring molecules.[16] Most of the organic acid complexes of rare earth metals possess the multi-core aggregation structures. For the Sm-La-pyridyl carboxylic acid systems, the crystal structures of complex molecules were changed with the addition of doping ion La(III). Meanwhile, there may be two molecular structures existing in those doping groups: heterometallic complexes and encapsulated structures made by doping ion complexes packaging the central metal compounds.[17]

In the heterometallic structures, the energy absorbed by ligands combination with Sm(III) was released in the form of central ion luminescence. However, energy absorbed by ligands joined to the inertia ion La(III) was not consumed by radiation due to the high excited state energy level induced by stable electronic structure of La(III), but it was transferred by intramolecular energy transfer to Sm(III) that shared the same ligand with La(III), then lost by Sm(III) in the form of light, so that the probability of characteristic fluorescence emission of Sm(III) was higher and the emission intensity was improved greatly. With reference to the encapsulated structures, La(III)-centered ligands absorbed the energy to reach the lowest excited triplet state, yet the energy was diverted to neighboring ligands coordinated with Sm(III) by Forster energy transfer rather than to doping La(III) with stable electronic structure, which made Sm(III) get more energy sources. Meanwhile, the addition of doping ion reduced the concentration of the coordinated Sm(III), which weakened the so-called "concentration quenching", accordingly, the characteristic fluorescence intensity of Sm(III) was also enhanced. On the other hand, the energy-absorption sections of the Sm-pyridyl carboxylic acid complexes were lessened with the addition of foreign ion La(III), resulting in the degenerated luminescent properties.[17,18]

The co-luminescence phenomenon was determined by the above two reasons. When the mole fractions of La(III) were lower than the optimal level for each system, the first reason became the major factor, leading to the markedly increase of fluorescence intensity; while the second one became the dominant aspect when continuously increasing amount of La(III).

BSA Binding Studies.

Interaction of the Selected Complex with BSA: To a 5 mL of calorimetric tube, 0.3 mL BSA stock solution, 1 mL Tris-HCl buffer solution and 1 mL $K_4Sm_{0.4}La_{0.6}(\mathbf{L}_4)Cl_3{\cdot}5H_2O$ working solution (concentration: 0-16 × 10^{-6} mol·L^{-1}) were added in turn, and 5 mL NaCl was added successively. The mixture was incubated for 10 min at room temperature. Subsequently, the fluorescence of the mixture was measured (excitation at 280 nm, emission wavelengths at 300-600 nm and slit widths of 5 nm) at 293 K, 301 K, and 309 K, respectively.

Main Quenching Mechanism of BSA by the $K_4Sm_{0.4}La_{0.6}(\mathbf{L}_4)Cl_3{\cdot}5H_2O$: At the excitation wavelength of 280 nm, the fluorescence spectra of BSA with varying concentrations of $K_4Sm_{0.4}La_{0.6}(\mathbf{L}_4)Cl_3{\cdot}3H_2O$ at 293 K are shown in Figure 3. The naturally fluorescence of BSA at around 340 nm was gradually quenched along with the increasing concentration of $K_4Sm_{0.4}La_{0.6}(\mathbf{L}_4)Cl_3{\cdot}5H_2O$ and a slight blue shift of the emission maximum wavelength was observed. Truths above indicate that there are strong interactions and radiationless energy transfer between $K_4Sm_{0.4}La_{0.6}(\mathbf{L}_4)Cl_3{\cdot}5H_2O$ and protein.[19,20]

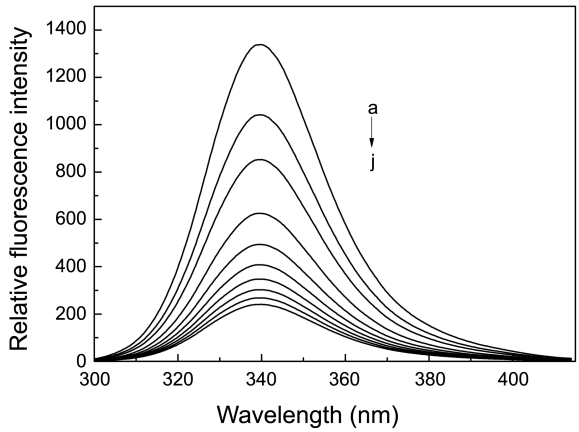

Figure 3. Effect of $K_4Sm_{0.4}La_{0.6}(\mathbf{L}_4)Cl_3{\cdot}5H_2O$ concentration on fluorescence spectrum of BSA (T = 293 K, pH = 7.4, λ_{ex} = 280 nm. a-j, c(BSA) = 1.0 × 10^{-6} mol·L^{-1}, c($K_4Sm_{0.4}La_{0.6}(\mathbf{L}_4)Cl_3{\cdot}5H_2O$) /($10^{-6}$ mol·L^{-1}): 0, 1.0, 2.0, 4.0, 6.0, 8.0, 10.0, 12.0, 14.0, and 16.0, respectively).

In given conditions (such as fixed pH, temperature and ionic strength), fluorescence quenching may result from ground complex formation, energy transfer and dynamic quenching processes.[21] Dynamic quenching is a process that the fluorophore and the quencher come into contact during the lifetime of the excited state, whereas static quenching refers to fluorophore-quencher complex formation.[22] Fluorescence quenching data can be analyzed by the *Stern-Volmer* equation[23]:

$$F_0/F = 1 + K_{sv}[Q] = 1+\tau_0 k_q [Q] \quad (1)$$

Where, F_0 and F are the fluorescence intensities in the absence and presence of quencher, respectively. K_{sv} is the *Stern-Volmer* quenching constant, $[Q]$ the concentration of quencher, and τ_0 the average fluorescence lifetime of biomolecule about 10^{-8} s.[24] k_q is the biomolecule quenching rate constant and the value of the maximum scattering collision quenching constant is 2.0×10^{10} mol^{-1}·s^{-1}.[25] Figure 4 shows the *Stern-Volmer* plots of BSA quenched by $K_4Sm_{0.4}La_{0.6}$-(**L**$_4$)Cl_3·$5H_2O$, in which the F_0/F versus $[Q]$ at three temperatures is given.

The values of K_{sv} and correlation coefficient R^2 are outlined in Table 3. The values of k_q are much larger than those of the maximum scattering collision quenching constant and the slope of the *Stern-Volmer* plot are inversely correlated with the temperature, which indicate that the main quenching mechanism of BSA by $K_4Sm_{0.4}La_{0.6}$(**L**$_4$)Cl_3·$3H_2O$ should be a static quenching procedure.[22]

Binding Constants and Binding Sites: As is discussed above, the fluorescence quenching coming from the complex formation between protein and quencher is static quenching process. The relationship between fluorescence intensity and the concentration of quenchers can be described by the following Eq. (2) for static quenching[26]:

$$\log[F/(F_0-F)] = \log\frac{1}{K_a} + n\log\frac{1}{[Q]} \quad (2)$$

Where, K_a and n are the binding constant and the number of binding site, respectively.

From Eq. (2), the binding parameters at different temperatures can be obtained by a plot of $\log[F/(F_0-F)]$ versus $\log 1/[Q]$ (seen in Figure 5).

As is expressed in Table 4, the value of K_a is rather larger than the free ligand **L**$_4$ reported by Tang R. R.,[13] indicating that the addition of the rare earth ion to the **L**$_4$ center is helpful to the binding of BSA. The values of n approximately equal to 1.0 indicate there was one independent class of binding site on BSA for complex.

Thermodynamic Parameters and Nature of the Binding Forces: In general, the interaction forces between proteins and ligands may include hydrophobic, hydrogen bonds, van der Waals, electrostatic interactions, *etc*. To

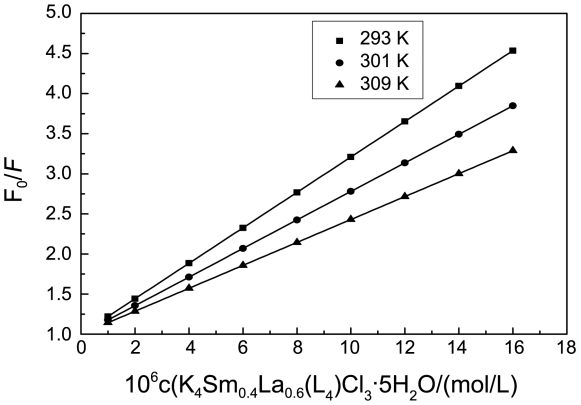

Figure 4. The *Stern-Volmer* curves of BSA quenched by $K_4Sm_{0.4}La_{0.6}$(**L**$_4$)Cl_3·$5H_2O$.

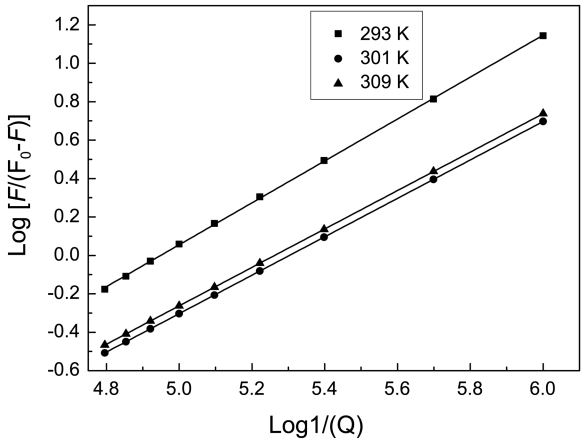

Figure 5. Plots of $K_4Sm_{0.4}La_{0.6}$(**L**$_4$)Cl_3·$5H_2O$ quenching effect on BSA fluorescence at different temperatures.

Table 4. The binding constants K_a and binding sites n at different temperatures for $K_4Sm_{0.4}La_{0.6}$(**L**$_4$)Cl_3·$5H_2O$ -BSA system

T (K)	K_a ($\times 10^5$ L·mol^{-1})	n	$^aR^2$
293	2.50	1.09	0.99997
301	2.01	1.00	0.99999
309	1.83	0.98	0.99999

^aR is the correlation coefficient.

Table 3. Fluorescence quenching constants and thermodynamic parameters of $K_4Sm_{0.4}La_{0.6}$(**L**$_4$)Cl_3·$5H_2O$-BSA system at different temperatures

pH	T (K)	K_{sv} ($\times 10^5$ L·mol^{-1})	k_q ($\times 10^{13}$ L·mol^{-1}·S^{-1})	$^aR^2$	ΔH (kJ·mol^{-1})	ΔS (J·mol^{-1}·K^{-1})	ΔG (kJ·mol^{-1})	$^bR^2$
7.4	293	2.85	2.85	0.99999	-14.59	53.48	-30.25	0.99993
	301	2.01	2.01	0.99998			-30.69	
	309	1.83	1.83	0.99998			-31.12	

^aR is the correlation coefficient of the value of K_{sv}. ^bR is the correlation coefficient of the value of ΔH, ΔS.

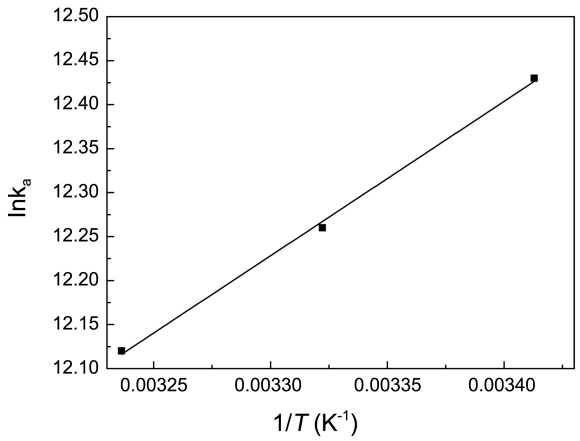

Figure 6. Van't Hoff plot of the interaction of BSA and $K_4Sm_{0.4}La_{0.6}(\mathbf{L}_4)Cl_3{\cdot}5H_2O$.

elucidate the interaction of $K_4Sm_{0.4}La_{0.6}(\mathbf{L}_4)Cl_3{\cdot}3H_2O$ with BSA, the thermodynamic parameters (ΔH, ΔS) were calculated from the Van't Hoff equation (Eq. 3) at three different temperatures.

$$\ln K_a = -\Delta H/RT + \Delta S/R \quad (3)$$

Where, K_a is the effective binding constant at the corresponding temperature. R is the universal gas constant. ΔH is enthalpy change and ΔS entropy change. If the enthalpy change (ΔH) does not vary significantly at the temperature range studied, ΔH can be regarded as a constant. Figure 6 gives the Van't Hoff plot of the interaction of BSA and $K_4Sm_{0.4}La_{0.6}(\mathbf{L}_4)Cl_3{\cdot}5H_2O$.

The value of ΔH and ΔS can be calculated from the slope and intercept of the line, respectively. The free energy change (ΔG) was estimated from Eq. (4).

$$\Delta G = \Delta H - T\Delta S \quad (4)$$

The negative values of free energy (ΔG), seen in Table 3, supports the assertion that the binding process is spontaneous. When $\Delta H < 0$ or $\Delta H \approx 0$, $\Delta S > 0$, the main acting force is electrostatic force; when $\Delta H > 0$, $\Delta S > 0$, the main acting force is van der Waals or hydrogen bond and when $\Delta H > 0$, $\Delta S > 0$, the main force is hydrophobic.[27] The enthalpy (ΔH) and entropy (ΔS) values of the interaction between $K_4Sm_{0.4}La_{0.6}(\mathbf{L}_4)Cl_3{\cdot}5H_2O$ and BSA indicate that electrostatic force played major roles in the binding reaction.

Conclusions

In this paper, a novel luminescent ligand $\mathbf{L}_1$ has been synthesized. The study of co-luminescence properties validated Sm-La-$\mathbf{L}_1$, Sm-La-$\mathbf{L}_3$, Sm-La-$\mathbf{L}_4$ were comparatively excellent co-luminescence systems, whose maximum fluorescence intensity was up to 7176, 10760, 14043, when the mole fractions of La(III) in mixed ions were 0.6, 0.3, 0.6, respectively. The fluorescence quenching results demonstrated the fluorescence quenching mechanism of BSA initiated by $K_4Sm_{0.4}La_{0.6}(\mathbf{L}_4)Cl_3{\cdot}5H_2O$ was a static quenching process. The binding constants were rather larger than the free ligand and the number of binding sites was equal to 1.0 at different temperatures. The values of thermodynamic parameters confirmed the electrostatic force played major role in the binding reaction. The results are expected to give important insight into interactions of the rare earth complexes and BSA, which showed the reference value for a model of application for drug design.

Acknowledgments. Financial support from the National Natural Science Foundation of China (No. 21071152) is gratefully acknowledged.

References

1. Eliseeva, S. V.; Claude, J.; Bünzli, G. *Chem. Rev.* **2010**, *39*, 189.
2. de Sá, G. F.; Malta O. L.; de Mello Donegá, C.; Simas, A. M.; Longo, R. L.; Santa-Cruz, P. A.; da Silva, E. F., Jr. *Coord. Chem. Rev.* **2000**, *196*, 165.
3. Li, Y.; Zhao, Y. L. *J. Fluoresc*. **2009**, *19*, 641.
4. Chen, J.; Selvin, P. R. *J. Photochem. Photobiol. A* **2000**, *135*, 27.
5. Nurchi, V.; Crisponi, G.; Ganadu, M. L. *Anal. Chim. Acta* **1990**, *239*, 157.
6. Gu, G. L.; Tang, R. R.; Zheng, Y. H.; Shi, X. M. *Spectrochim. Acta, Part A* **2008**, *71*, 209.
7. Adams, M. J.; Highfield, J. G.; Kirkbright, G. F. *Anal. Chem.* **1980**, *52*, 1260.
8. Yang, J. H.; Zhu, G. Y.; Wang, H. *Anal. Chim. Acta* **1987**, *198*, 287.
9. Ci, Y. X.; Lan, Z. H. *Analyst (Lond.)* **1988**, *113*, 1453.
10. Yang, Y. T.; Zhang, S. Y.; Su, Q. D. *Mater. Res. Bull.* **2005**, *40*, 1010.
11. Tang, R. R.; Zhao, Q.; Yan, Z. E.; Luo, Y. M. *Synth. Commn.* **2006**, *36*, 2027.
12. Tang, C. Q.; Tang, R. R.; Tang, C. H.; Zeng, Z. W. *Bull. Korean Chem. Soc.* **2010**, *31*, 2.
13. Tang, R. R.; Tang, C. H.; Tang, C. Q. *J. Organomet. Chem.* **2011**, *696*, 2040.
14. Xiong, B. K. *J. Chin. Rare Earth Soc.* **1994**, *12*, 265.
15. Olson, R. E.; Christ, D. D. *Annu. Rep. Med. Chem.* **1996**, *31*, 327.
16. Li, L.; Yang, J. H.; Wu, X.; Sun, C. X. *J. Lumin.* **2003**, *101*, 141.
17. Zhou, Z. C.; Shu, W. G.; Ruan, J. M.; Huang, B. Y. *Rare Met.* **2004**, *23*, 306.
18. Tao, D. L.; Zhang, T.; Xu, Y. Z.; Xu, Z.; Gao, X.; Zhang, Y. P.; Xu, J. G.; Xu, X. R. *J. Chin. Rare Earth. Soc.* **2001**, *19*, 543.
19. Guo, C. C.; Li, H. P.; Zhang, X. B.; Tong. X. B. *Chem. J. Chinese Univ.* **2003**, *24*, 282.
20. Wang, J.; Liu, L.; Liu, B.; Guo, Y.; Zhang, Y.; Xu, R.; Wang, S.; Zhang, X. *Spectrochim. Acta. Part A* **2010**, *75*, 366.
21. Bhattacharyya, M.; Chaudhuri, U.; Poddar, R. K. *Biochem. Biophys. Res. Commun.* **1990**, *167*, 1146.
22. Guo, J.; Han, X. W.; Tong, J.; Guo, C.; Yang, W. F.; Zhu, J. F.; Fu, B. *J. Mol. Struct.* **2010**, *966*, 129.
23. Liu, Y. C.; Yang, Z. Y. *J. Organomet. Chem.* **2009**, *694*, 3091.
24. Zhou, N.; Liang, Y. Z.; Wang, P. *J. Photochem. Photobio. A: Chem.* **2007**, *185*, 271.
25. Ware, W. R. *J. Phys. Chem.* **1962**, *66*, 455.
26. Kang, J.; Liu, Y.; Xie, M. X.; Li, S.; Jiang, M.; Wang, Y. D. *BBA-Gene Subjects.* **2004**, *1674*, 205.
27. Sun, Y. T.; Zhang, H. T.; Sun, Y.; Zhang, Y. P.; Liu, H.; Cheng, J. H.; Bi, S. Y.; Zhang, H. Q. *J. Lumin.* **2010**, *130*, 270.